9th AIAA/ASME Joint Thermophysics and Heat Transfer Conference
San Francisco, CA, 5-8 June 2006 AIAA 2006-2927

Multiphysics Analysis of a Solid-Core Nuclear Thermal Engine Thrust Chamber

Ten-See Wang*, Francisco Canabal†
NASA Marshall Space Flight Center, Huntsville, Alabama, 35812
Gary Cheng‡
University of Alabama, Birmingham, Alabama, 35294
Yen-Sen Chen§
Engineering Sciences, Inc., Huntsville, Alabama, 35815

The objective of this effort is to develop an efficient and accurate thermo-fluid computational methodology to predict environments for a hypothetical solid-core, nuclear thermal engine thrust chamber. The computational methodology is based on an unstructured-grid, pressure-based computational fluid dynamics methodology. Formulations for heat transfer in solids and porous media were implemented and anchored. A two-pronged approach was employed in this effort: A detailed thermo-fluid analysis on a multi-channel flow element for mid-section corrosion investigation; and a global modeling of the thrust chamber to understand the effect of hydrogen dissociation and recombination on heat transfer and thrust performance. The formulations and preliminary results on both aspects are presented.

Nomenclature

C_1, C_2, C_3, C_μ = turbulence modeling constants, 1.15, 1.9, 0.25, and 0.09.
C_p = heat capacity
D = diffusivity
F = empirical multiplier
H = total enthalpy
K = thermal conductivity
k = turbulent kinetic energy
L = drag loss due to porous media
p = pressure
Q = heat flux or heat source
Q = heat source due to porous media
T = temperature
t = time, s
U = flow speed
u_i = mean velocities in three directions
x = Cartesian coordinates
α = species mass fraction
β = porosity or void of fraction
ε = turbulent kinetic energy dissipation rate

*Technical Assistant, ER43, Thermal and Combustion Analysis Branch, Propulsion Structure, Thermal, and Fluids Analysis Division, Senior Member AIAA.
† Project Engineer, EV33, Aerosciences Branch, Structural Design and Analysis Division, Member AIAA.
‡Assistant Professor, Department of Mechanical Engineering, Member AIAA.
§President, Member AIAA.

θ = energy dissipation contribution
μ = viscosity
μ_t = turbulent eddy viscosity ($=\rho C_\mu k^2/\varepsilon$)
Π = turbulent kinetic energy production
ρ = density
σ = turbulence modeling constants
τ = shear stress
ω = chemical species production rate

Subscripts and superscripts

cl = centerline
s = surface or solid
t = turbulent flow
v = volume

I. Introduction

Nuclear thermal propulsion can carry far larger payloads and reduce travel time for astronauts traveling to Mars than is now possible with chemical propulsion. One of the Concepts that was extensively tested during the Rover/NERNA era and appear to be the most feasible is the solid-core concept.[1] This concept involves a solid-core reactor consisting of hundreds of heat generating solid flow elements, and each flow element containing tens of flow channels through which the working fluid hydrogen acquires energy and expands in a high expansion nozzle to generate thrust. The solid-core reactor is therefore nothing but a heat exchanger. To minimize the effect of its weight, the reactor often operates at very high temperature and power density, which imposes real challenges to the integrity of the flow element material. To make the solid-core reactor a viable concept for Mars missions, we must understand the effect of hydrogen as a high temperature working fluid and develop materials that withstand the harsh flow element environment.

The advantage of hydrogen as a propellant is well known due to its low molecular weight. The effect of hydrogen as a working fluid in a nuclear heat exchanger however, is not well studied. As a rule of thumb, hydrogen decomposes to form hydrogen atoms as temperature increases and hydrogen atoms recombine to become hydrogen molecule as temperature decreases. Capturing that feature with finite-rate chemistry calculation, Wang, et al. reported that a decomposing hydrogen jet maintains a higher stagnation temperature than that of a frozen hydrogen jet while the jets impinging on a cylindrical specimen, inside a water-cooled tester.[2] This suggests a higher heat transfer efficiency of hydrogen atom over that of hydrogen molecule. Also, since the formula weight of a hydrogen atom is half that of a hydrogen molecule, it has been speculated that high concentration of hydrogen atoms would increase the thrust performance, thereby suggesting higher reactor operating temperatures. However, hydrogen atoms recombine to form hydrogen molecule as temperature decreases in the expansion nozzle, meaning the hydrogen atoms gained in the reactor may be lost in the nozzle.

One of the impacts of operating at the combination of high temperature and high power density is a phenomenon known as the mid-section corrosion, as reported during the legacy engine tests.[1, 3] It is an excessive mass loss of the flow element material near the mid-section during testing. The symptom was cracked coating layer while the purpose of coating was to isolate the carbonaceous compound in the flow element matrix from the attack by hydrogen. The causes of mid-section corrosion were speculated as a mismatch in the thermal expansion of flow element and its coating material, high flow element web internal temperature gradients, and change of solid thermal property due to irradiation.[4] Note that another speculation was that the flow was choked in the long flow channels of the flow element.

One way to help understanding the effect of hydrogen as a working fluid and developing materials that withstand the harsh environment is to develop computational methodology that can accurately predict thermal-fluid environments inside the nuclear thermal engine thrust chamber and reproduce the flow element thermal environment occurring in the legacy engine tests. The objective of this effort is therefore to develop an efficient and accurate multiphysics thermal-fluid computational methodology to predict environments for a hypothetical solid-core thrust chamber and the associated flow element, similar to those in the Small Engine.[1] The Small Engine was a paper engine designed near the end of the Rover/NERVA era and bears common features of other legacy engines tested during that time period, but was never built nor tested. The hypothetical thrust chamber and flow element, which are being redesigned by the System Analysis Group at Marshall Space Flight Center, consists of 564 flow elements and of 19 flow channels for each flow element, respectively. The computational methodology was based on an existing

Unstructured-grid Navier-Stokes Internal-external computational fluid dynamics Code (UNIC). Conjugate heat transfer formulations for coupling fluid dynamics and conductive heat transfer in solids and for flow and conductive heat transfer in porous media were developed and tested. A two-pronged approach was employed: a detailed analysis of the 19-channel flow element, and a global analysis of the entire thrust chamber. In the global thrust chamber analysis, the 19 channels for each flow element were lumped together as a porous media to save computational resources, and the core surrounding components such as the slats and reflector were treated as heat conducting solids to provide accurate boundary condition for the solid-core environment.

II. Computational Methodology

A. Computational Fluid Dynamics

The CFD methodology was based on a multi-dimensional, finite-volume, viscous, chemically reacting, unstructured grid, and pressure-based formulation. Time-varying transport equations of continuity, species continuity , momentum, total enthalpy, turbulent kinetic energy, and turbulent kinetic energy dissipation were solved using a time-marching sub-iteration scheme and are written as:

$$\frac{\partial \rho}{\partial t}+\frac{\partial}{\partial x_j}\left(\rho u_j\right)=0 \tag{1}$$

$$\frac{\partial \rho\alpha_i}{\partial t}+\frac{\partial}{\partial x_j}\left(\rho u_j\alpha_j\right)=\frac{\partial}{\partial x_j}\left[\left(\rho D+\frac{\mu_t}{\sigma_\alpha}\right)\frac{\partial \alpha_i}{\partial x_j}\right]+\omega_i \tag{2}$$

$$\frac{\partial \rho u_i}{\partial t}+\frac{\partial}{\partial x_j}\left(\rho u_j u_i\right)=-\frac{\partial p}{\partial x_i}+\frac{\partial \tau_{ij}}{\partial x_j} \tag{3}$$

$$\frac{\partial \rho H}{\partial t}+\frac{\partial}{\partial x_j}\left(\rho u_j H\right)=\frac{\partial p}{\partial t}+Q_r+\frac{\partial}{\partial x_j}\left(\left(\frac{K}{C_p}+\frac{\mu_t}{\sigma_H}\right)\nabla H\right)+\frac{\partial}{\partial x_j}\left(\left(\left(\mu+\mu_t\right)-\left(\frac{K}{C_p}+\frac{\mu_t}{\sigma_H}\right)\right)\nabla\left(V^2/2\right)\right)+\theta \tag{4}$$

$$\frac{\partial \rho k}{\partial t}+\frac{\partial}{\partial x_j}\left(\rho u_j k\right)=\frac{\partial}{\partial x_j}\left[\left(\mu+\frac{\mu_t}{\sigma_k}\right)\frac{\partial k}{\partial x_j}\right]+\rho\left(\Pi-\varepsilon\right) \tag{5}$$

$$\frac{\partial \rho \varepsilon}{\partial t}+\frac{\partial}{\partial x_j}\left(\rho u_j \varepsilon\right)=\frac{\partial}{\partial x_j}\left[\left(\mu+\frac{\mu_t}{\sigma_\varepsilon}\right)\frac{\partial \varepsilon}{\partial x_j}\right]+\rho\frac{\varepsilon}{k}\left(C_1\Pi-C_2\varepsilon+C_3\Pi^2/\varepsilon\right) \tag{6}$$

A predictor and corrector solution algorithm was employed to provide coupling of the governing equations. A second-order central-difference scheme was employed to discretize the diffusion fluxes and source terms. For the convective terms, a second-order upwind total variation diminishing difference scheme was used. To enhance the temporal accuracy, a second-order backward difference scheme was employed to discretize the temporal terms. Details of the numerical algorithm can be found in Ref's 5-9.

An extended k-ε turbulence model[10] was used to describe the turbulence. A modified wall function approach was employed to provide wall boundary layer solutions that are less sensitive to the near-wall grid spacing. Consequently, the model has combined the advantages of both the integrated-to-the-wall approach and the conventional law-of-the-wall approach by incorporating a complete velocity profile and a universal temperature profile[6]. A 2-species, 3-reaction detailed mechanism[11] was used to describe the hydrogen dissociation and recombination chemical kinetics.

B. Heat Transfer in Solids

The solid heat conduction equation was solved with the gas-side heat flux distributions as its boundary conditions. The solid heat conduction equation can be written as:

$$\frac{\partial \rho C_p T}{\partial t}=\frac{\partial}{\partial x_j}\left(K\frac{\partial T}{\partial x_i}\right)+Q_v+Q_s \tag{7}$$

C. Flow and Heat Transfer in Porous Media

A two-temperature porosity model was formulated and separate thermal conductivities for the flow and the solid parts were used. The heat transfer between the flow and solid was modeled by using the empirical correlation of heat transfer coefficient for circular pipes as a function of flow Reynolds number. Empirical multipliers for both the heat transfer and drag loss will be determined by comparing solutions of flow passing through a porous flow element with those of a 19-channel flow element using detailed conjugate heat transfer modeling. The only affected fluid governing equations are Navier-Stokes and energy equations and can be rewritten as:

$$\frac{\partial \rho u_i}{\partial t}+\frac{\partial}{\partial x_j}\left(\rho u_j u_i\right)=-\frac{\partial p}{\partial x_i}+\frac{\partial \tau_{ij}}{\partial x_j}-\frac{L}{\beta} \tag{8}$$

$$\frac{\partial \rho H}{\partial t}+\frac{\partial}{\partial x_j}\left(\rho u_j H\right)=\frac{\partial p}{\partial t}+Q_r+\frac{\partial}{\partial x_j}\left(\left(\frac{K}{C_p}+\frac{\mu_t}{\sigma_H}\right)\nabla H\right)+\frac{\partial}{\partial x_j}\left(\left(\left(\mu+\mu_t\right)-\left(\frac{K}{C_p}+\frac{\mu_t}{\sigma_H}\right)\right)\nabla\left(V^2/2\right)\right)+\theta+\frac{Q_s}{\beta} \tag{9}$$

For the solid heat conduction in porous media,

$$\frac{\partial \rho_s C_{ps} T_s}{\partial t}=\frac{\partial}{\partial x_j}\left(K_s\frac{\partial T_s}{\partial x_i}\right)+\frac{Q_v+Q_s}{1-\beta} \tag{10}$$

For the present 19-channel flow elements heat exchanger configuration, drag loss in circular pipes can be used as a point of departure. That is,

$$L=\frac{1}{2}\rho\, c_f |U|\bullet u_i \tag{11}$$

where $c_f = 0.0791\mathrm{Re}^{-0.25}$

For the heat exchange source term,

$$Q_s=\frac{1}{2}\rho\frac{c_f}{p_r^{2/3}}|U|\,C_p\left(T_s-T\right)f \tag{12}$$

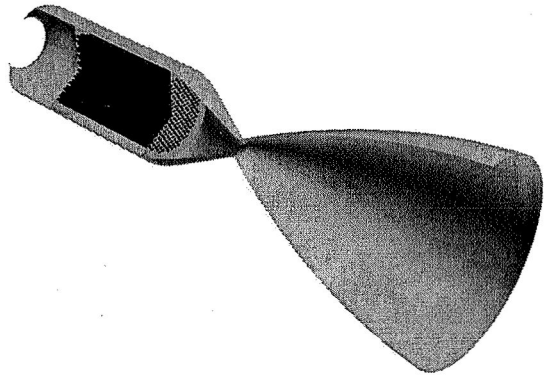

Fig. 1 Computational geometry representation of a solid-core nuclear thermal thrust chamber.

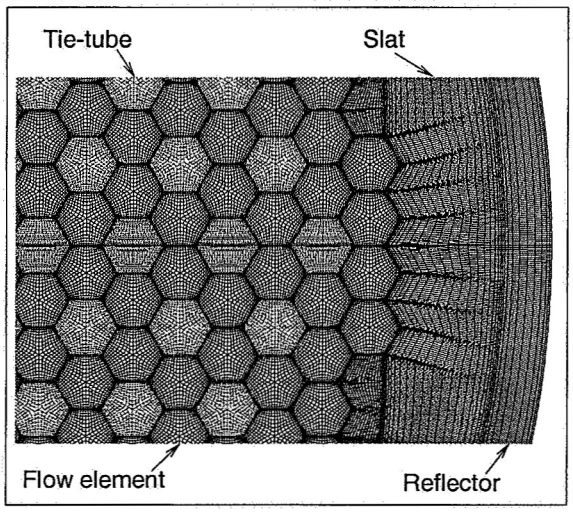

Fig. 2 Computational grid layout of the flow element, tie-tubes, slat, and reflector.

where f is an empirical parameter to be identified by comparing solutions of the porosity model and the 19-channel conjugate heat transfer model.

III. Computational Grid Generation

Hybrid computational grids were generated using a software package GRIDGEN[12] for both detailed flow element and global thrust chamber analyses. There are 564 flow elements and 241 support elements or tie-tubes in the solid-core. The hexagonal flow elements have 19 coolant channels and the support elements have one large hole. Each flow element is held in position by three support elements and the corresponding hot-end support system (not modeled). Due to geometrical symmetry, a 30 deg. Cut of the thrust chamber was solved. Figure 1 shows a computational geometry representation of the thrust chamber and tie-tube walls, while Fig. 2 shows a partial cross-sectional cut of the solid-core depicting flow elements, tie-tubes, slat, and reflector.

Figure 3 shows a computational grid representation of a quarter of a 19-channel flow element. Due to symmetry, only a quarter of a flow element was solved. Figure 2 shows the surface grid representation of the web of a 19-channel flow element. This web grid is only used for identifying the physical conjugate heat transfer region in Fig. 3 where the actual computational grid is shown. These grids were used to study the mid-section corrosion phenomenon. Similar, but shorter grids were used to establish porosity model suitable in describing the effects of drag and heat transfer of the 19-channel flow elements, which was used to model the flow and heat transfer in the flow elements of the solid-core of the global thrust chamber (figs. 1 and 2).

The global thrust chamber grid shown in Figs 1 and 2 consists of 7,460,255 nodal points, or 8,932,018 computational cells.

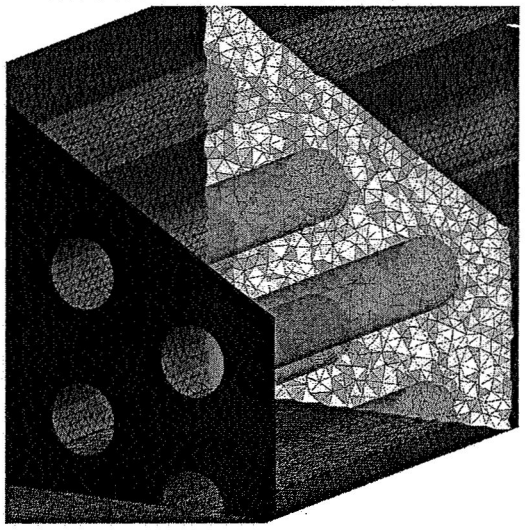

Fig. 3 A computational grid layout of a quarter of a 19-channel flow element.

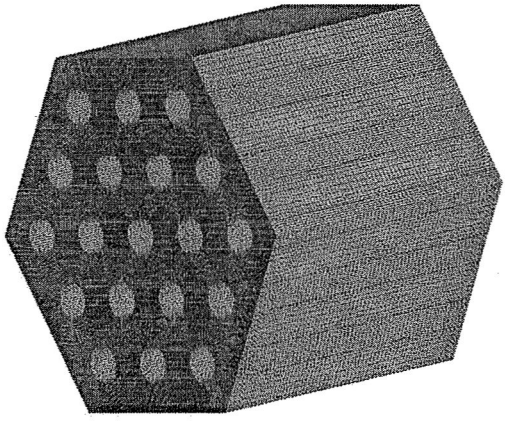

Fig. 4 Surface grid representation for the web of a 19-channel flow element.

IV. Boundary and Inlet Conditions

No-slip condition was applied to the solid walls and fixed mass flow rate boundary condition was used at the inlet. Mass conservation boundary condition was used at the exit for the detailed 19-channel, single flow element analysis, while supersonic outflow boundary condition was applied at the nozzle exit for the global thrust chamber analysis.

In the global thrust chamber analysis, the inlet conditions were obtained from a system model simulation; for the outside chamber walls, a far-field temperature of 400 K was specified to convey heat out to the ambience. For simplicity, the minor thermal effect of the tie-tubes was not modeled, since that effect is included in the inlet flow from system simulation. Adiabatic wall boundary condition was therefore used for the tie-tube walls.

In the 19-channel, single flow element analysis, conduction heat transfer was applied to the web. In the global thrust chamber analysis, conduction heat transfer was applied to both the reflector and slat regions, while porosity modeling was applied to the core of flow elements.

As to the nuclear power, since it was known that the power distribution inside a solid-core reactor takes the shape of a Cosine curve; the power peaks at the center of the core and reduces to a small value at the core boundaries due to escaping neutrons. A Cosine power profile was numerically imposed to the core of the global thrust chamber to simulate the effect of neutronics in all three directions. For a 19-channel, single flow element, a Cosine curve was applied in the flow direction, while a clipped Cosine curve was applied in the transverse direction.

V. Preliminary Results and Discussion

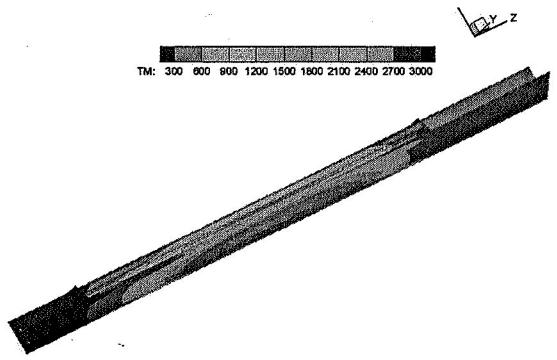

Fig. 5 Computed temperature contours for a 1/8 full-length single flow element.

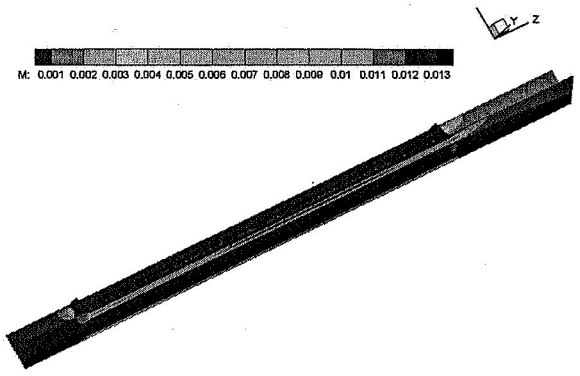

Fig. 6 Computed Mach number contours for a 1/8 full-length single flow element.

A. Detailed 19-channel, single flow element analysis

The goal of this analysis is to provide flow and thermal environments in order to understand and prevent mid-section corrosion issue, from both flow and thermal points of view. Figures 5 and 6 show the preliminary computed temperature and Mach number contours for a 1/8 full-length single flow element. From Fig. 5, it can be seen that the temperature contours resemble that of a Cosine distribution – a result of the assumed Cosine power distribution profile. From Fig. 6, it can be seen that the cold hydrogen picks up energy from the web and the flow Mach number increases. The computation of this 1/8 full-length single flow element and another for a full-length single flow element, are in progress. It is anticipated that the computed thermal environment for the full-length single flow element will show strong thermal gradients in both the axial and transverse directions on the web, especially in the coating region adjacent to the flow channel. It is also anticipated that the computed flow Mach number contours will reveal if the heat addition to the hydrogen in a long channel resulting in choked flow – a source of possible flow instability.

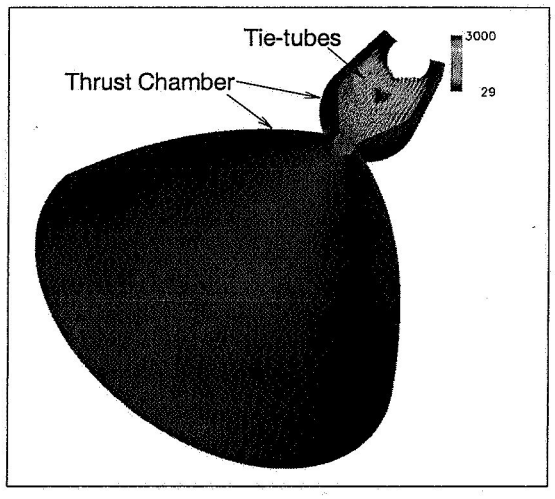

Fig. 7 Computed temperature contours on thrust chamber and tie-tube walls.

B. Global thrust chamber modeling

The goals of this analysis are to simultaneously provide thermal and flow environments for the entire thrust chamber, and to provide thrust performance with a unified analysis. The computation is in progress. Similar to the situations occurring in the powered single flow element computations, full power level cannot be applied at once. Otherwise, the rapid rise in temperature would result in a rapid rise in

pressure in the flow channel and the hydrogen gas cannot pass through, resulting in even rapid temperature rise and eventually the core temperature runaway. A gradual step-wise power ramp up procedure is being devised and tested. Since this is a unified analysis, the effects of hydrogen dissociation on heat transfer efficiency in the solid core and of hydrogen recombination in the nozzle on the eventual thrust performance can be investigated. Figure 7 shows the computed temperature contours on thrust chamber and tie-tube walls. It can be seen that the higher temperature in the solid-core as a result of the imposed Cosine power profile.

VI. Summary

A multiphysics thermo-fluid computational methodology was developed to predict environments for a hypothetical solid-core, nuclear thermal nuclear thrust chamber and for its flow element. A two-pronged approach is employed in this effort: A detailed conjugate heat transfer analysis on a multi-channel flow element, and a global modeling of the thruster chamber with a combined porosity modeling and conjugate heat transfer technique. It is anticipated that the detailed analysis on a single flow element provides detailed fluid, thermal, and hydrogen environments for better understanding of the mid-section corrosion phenomenon, while the global thrust chamber analysis helps the understanding of the simultaneous effects of hydrogen dissociation in the solid-core and hydrogen recombination in the nozzle on thrust performance.

Acknowledgments

This study was partially supported by a Nuclear Systems Office task entitled "Multiphysics Thrust Chamber Modeling" of which Wayne Bordelon was the project manager. Steve Simpson and Karl Nelson provided nozzle geometry and operating conditions for the hypothetical nuclear thermal engine. Bill Emrich suggested the Cosine power profile. Thermal properties provided by Panda Binayak, Robert Hickman, and Bill Emrich are also acknowledged.

References

[1]Koenig, D.R., "Experience Gained from the Space Nuclear Rocket Program (Rover)," LA-10062-H, Los Alamos National Laboratory, Los Alamos, New Mexico, 1986.

[2]Wang, T.-S., Foote, J., and Litchford, R., "Multiphysics Thermal-Fluid Design Analysis of a Non-Nuclear Tester for Hot-Hydrogen Material Development," Space Technology and Applications International Forum (STAIF-2006), Albuquerque, NM, Fe. 12-16, 2006, American Institute of Physics Proceedings, edited by El-Genk, M.S., Melville, N.Y., Vol. 813, 2006, pp. 537-544.

[3]Lyon, L.L., "Performance of (U,Zr)C-Graphite (Composite) and of (U,Zr)C (Carbide) Fuel Elements in the Nuclear Furnace 1 Test Reactor," LA-5398-MS, Los Alamos Scientific Laboratory, Los Alamos, New Mexico, 1973.

[4]Wang, T.-S., Luong, V., Foote, J., Litchford, R., and Chen, Y.-S., "Analysis of a Cylindrical Specimen Heated by an Impinging Hot Hydrogen Jet," AIAA Paper 2006-2926, 9th AIAA/ASME Joint Thermophysics and Heat Transfer Conference, San Francisco, CA, 2006.

[5]Chen, Y.-S., Liu, J., Zhang, S., and Mallapragada, P., "An Integrated Tool for Launch Vehicle Base-Heating Analysis," Final Report, NAS8-00002, Engineering Sciences, Inc., Huntsville, AL, 2001.

[6]Chen. Y.-S., Zhang S., and Liu, J., "Stage Separation Performance Analysis Project," Final Report, H-34345D, Engineering Sciences, Inc., Huntsville, AL, 2002.

[7]Wang, T.-S., Chen, Y.-S., Liu, J., Myrabo, L.N., and Mead, F.B. Jr., "Advanced Performance Modeling of Experimental Laser Lightcraft," *Journal of Propulsion and Power,* Vol. 18, No. 6, 2002, pp. 1129-1138.

[8]Wang, T.-S., "Multidimensional Unstructured-Grid Liquid Rocket Engine Nozzle Performance and Heat Transfer Analysis," *Journal of Propulsion and Power*, Vol. 22, No. 1, 2005, pp. 78-84.

[9]Wang, T.-S., "Transient 3-D Analysis of Nozzle Side Load in Regeneratively Cooled Engines," AIAA Paper 2005-3942, 41st AIAA/ASME/SAE/ASEE Joint Propulsion Conference, Tucson, Arizona, 2005.

[10]Chen, Y.-S., and Kim, S. W., "Computation of Turbulent Flows Using an Extended k-ε Turbulence Closure Model," NASA CR-179204, 1987.

[11]Wang, T.-S., "Thermophysics Characterization of Kerosene Combustion," *Journal of Thermophysics and Heat Transfer*, Vol. 15, No. 2, 2001, pp. 140-147.

[12]Steinbrenner, J.P., Chawner, J.R., and Fouts, C., "Multiple Block Grid Generation in the interactive Environment," AIAA Paper 90-1602, June 1990.

AIAA 2006-2927

Multiphysics Analysis of a Solid-Core Nuclear Thermal Engine Thrust Chamber

Ten-See Wang, Francisco Canabal
NASA Marshall Space Flight Center, Huntsville, AL 35812

Gary Cheng
University of Alabama, Birmingham, AL 35294

and
Yen-Sen Chen
Engineering Sciences, Inc., Huntsville, AL 35815

9th AIAA/ASME Joint Thermophysics and Heat Transfer Conference

San Francisco, CA, June 5-8, 2006

Acknowledgments

- This study was partially supported by a Nuclear Systems Office task entitled "**Multi-physics Thrust Chamber Modeling**".
- Steve Simpson and Karl Nelson provided nozzle geometry and operating conditions for the hypothetical nuclear thermal engine.
- Bill Emrich suggested the Cosine power profile.
- Panda Binayak, Robert Hickman, and Bill Emrich provided thermal properties for solids.

Introduction

- Nuclear thermal propulsion can carry larger payloads and reduce travel time to Mars than is now possible with chemical propulsion.
- Solid-core concept was extensively tested during the Rover/NERVA era and appears to be the most feasible.
- This concept involves a solid-core reactor consisting of hundred of heat generating flow elements, and each flow elements containing tens of flow channels through which the working fluid **hydrogen** acquires energy and expands in a high expansion nozzle to generate thrust.
- The solid-core reactor is a heat exchanger.
- The reactor often operates at **very high temperature and power density**, which imposes real challenges to the integrity of the flow element material.

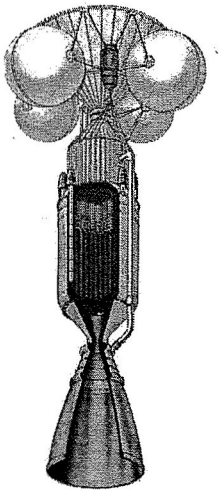

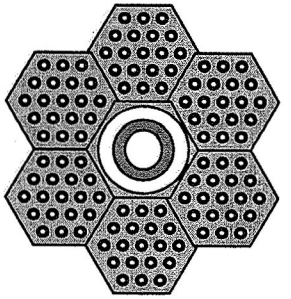

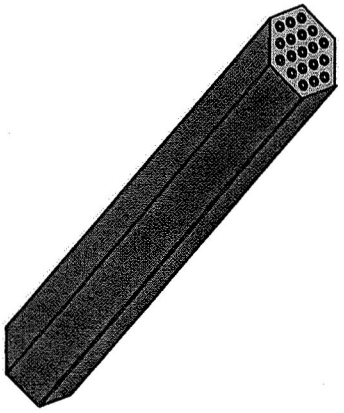

Introduction - continued

- Effect of hydrogen as a working fluid
  - Hydrogen is an excellent propellant
  - $H_2 = 2H$
  - Effect of hydrogen dissociation in core on heat transfer efficiency?
  - Hydrogen atom is a better propellant
  - Effect of hydrogen recombination in nozzle on thrust performance?
- Effect of hydrogen on flow element material
  - Hydrogen corrodes away channel walls and protective coatings made of certain materials
  - Corrosion enhances with higher temperature
  - Penetrates into fuel matrix core and weakens

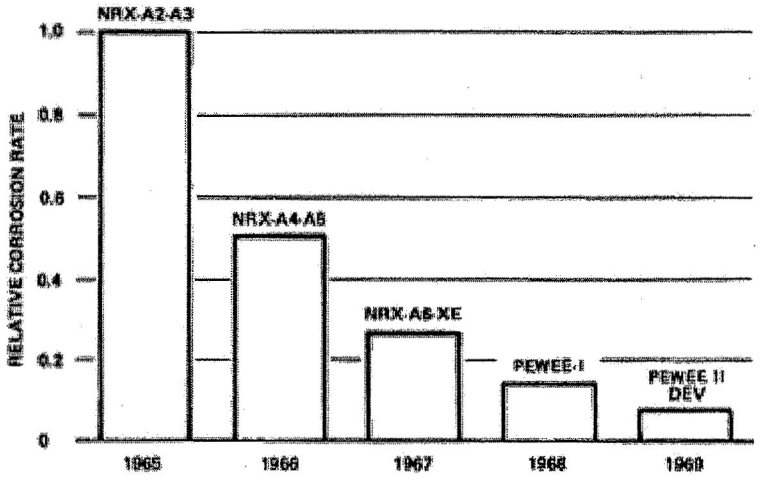

Introduction - continued

- Mid-section corrosion – cracked coating and excessive mass loss
- Causes of mid-section corrosion:
  - — Mismatch in the thermal expansion of flow element and its coating material
  - — Temperature difference between fuel and coating
  - — High flow element web internal temperature gradients, especially near the coating layer
  - — Change of solid thermal property due to irradiation
  - — Side load caused by flow choking in channels

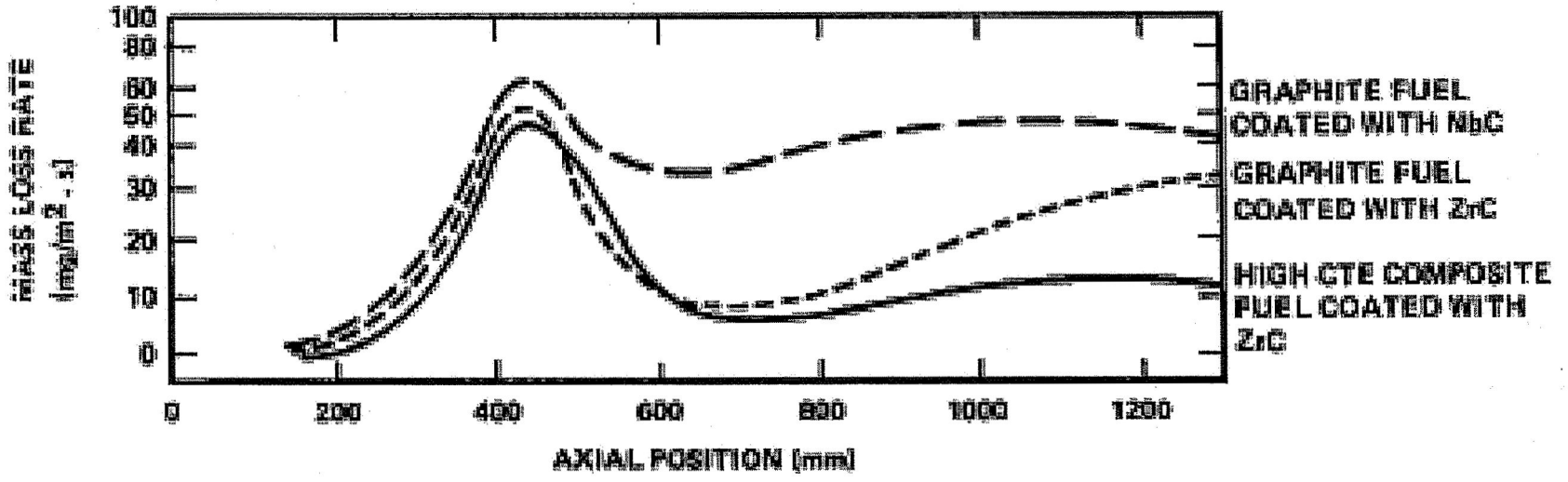

Introduction - continued

- To make solid-core nuclear thermal rocket a viable concept for Mars missions, we must
  - — Understand the effects of hydrogen as a working fluid on heat transfer efficiency in core and thrust performance in the nozzle
  - — Develop materials that withstand the harsh reactor environment
- One way to help understanding the effect of hydrogen as a working fluid and developing materials that withstand the harsh environment is to develop a computational methodology that can accurately predict thermal-fluid environments inside the thrust chamber and reproduce the flow element thermal environment occurring in the legacy engine tests.

Introduction - continued

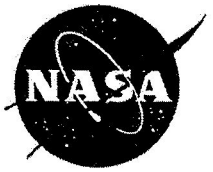

- The **objective** is to develop an efficient and accurate multiphysics thermo-fluid computational methodology to predict environments for a hypothetical solid-core thrust chamber and the associated flow element, similar to those in the **Small Engine**.
- The computational methodology was based on an existing CFD code (UNIC). Conjugate heat transfer formulations for coupling fluid dynamics and conductive heat transfer in solids and in porous media were developed and tested.

Introduction - continued

- The physics to be implemented into UNIC:
  - Conjugate heat transfer for flow and porous media (global multi-element thrust chamber)
    - is being anchored with computational analysis using a 19-channel single flow element configuration
  - Conjugate heat transfer for flow and solids (detailed multi-channel flow element)
    - Conjugate heat transfer with cylindrical specimen heated by impinging hot-hydrogen jet
      - Anchored with standard conductive heat transfer code SINDA.
      - Will be anchored with test data obtained from IR&D Focus Area Project "Hot Hydrogen Materials and Component Development".
    - Conjugate heat transfer with prescribed power distribution
      - Will be anchored with test data obtained from Task 12 – NTREES

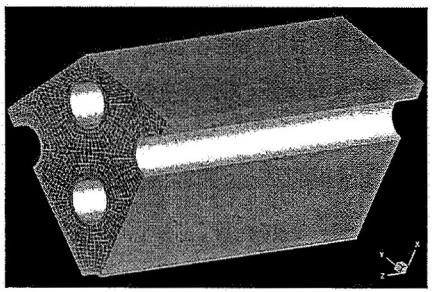

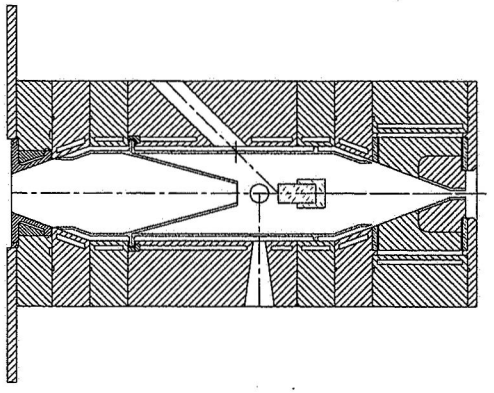

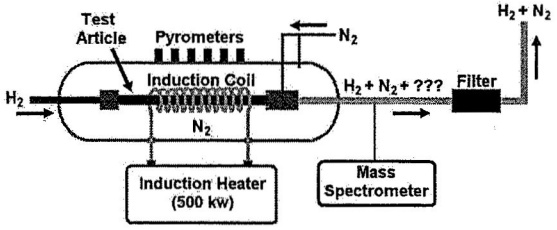

UNIC CFD code

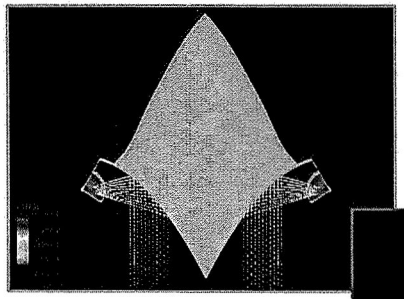

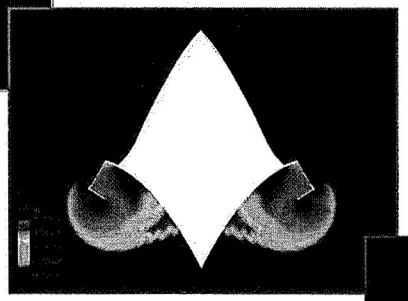

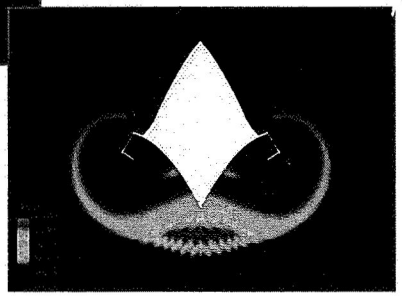

Transient Laser Lightcraft simulation

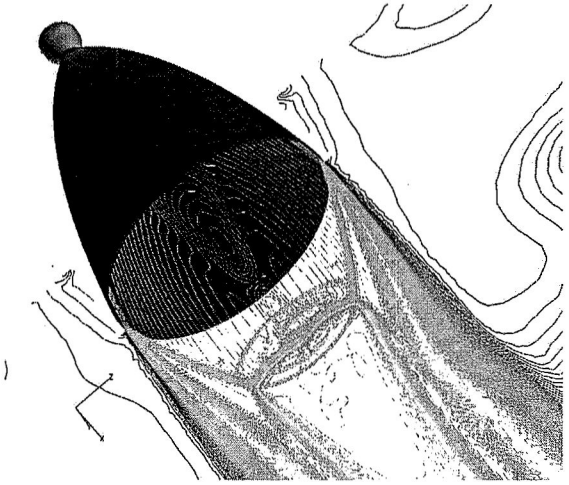

Transient SSME start-up and shut-down simulation

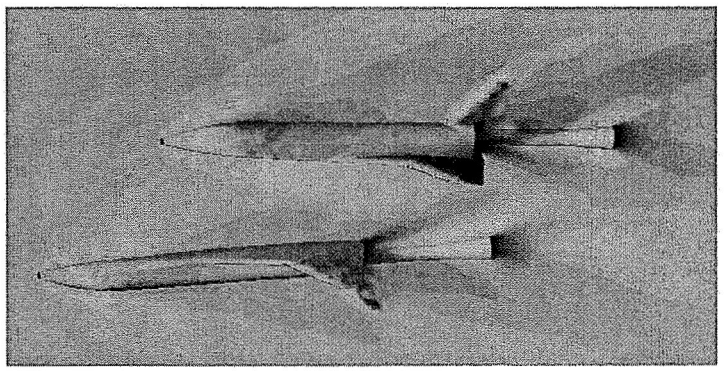

Transient stage separation

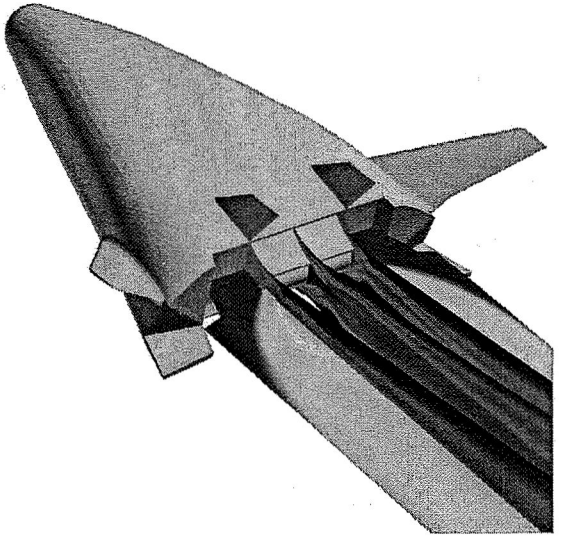

X33 plume induced base-heating during one power-pack out

UNIC Computational Methodology
Conjugate Heat Transfer: Gas-side Governing Equations

$$\frac{\partial \rho}{\partial t}+\frac{\partial}{\partial x_j}\left(\rho u_j\right)=0$$

$$\frac{\partial \rho \alpha_i}{\partial t}+\frac{\partial}{\partial x_j}\left(\rho u_j \alpha_j\right)=\frac{\partial}{\partial x_j}\left[\left(\rho D+\frac{\mu_t}{\sigma_\alpha}\right)\right]+\omega_i$$

$$\frac{\partial \rho u_i}{\partial t}+\frac{\partial}{\partial x_j}\left(\rho u_j u_i\right)=-\frac{\partial p}{\partial x_i}+\frac{\partial \tau_{ij}}{\partial x_j}$$

$$\frac{\partial \rho H}{\partial t}+\frac{\partial}{\partial x_j}\left(\rho u_j H\right)=\frac{\partial p}{\partial t}+Q_r+\frac{\partial}{\partial x_j}\left[\left(\frac{K}{C_p}+\frac{\mu_t}{\sigma_H}\right)\nabla H\right]+\frac{\partial}{\partial x_j}\left\{\left[\left(\mu+\mu_t\right)-\left(\frac{K}{C_p}+\frac{\mu_t}{\sigma_H}\right)\right]\nabla\left(\frac{V^2}{2}\right)\right\}+\theta$$

$$\frac{\partial \rho k}{\partial t}+\frac{\partial}{\partial x_j}\left(\rho u_j k\right)=\frac{\partial}{\partial x_j}\left[\left(\mu+\frac{\mu_t}{\sigma_k}\right)\frac{\partial k}{\partial x_j}\right]+\rho\left(\Pi-\varepsilon\right)$$

$$\frac{\partial \rho \varepsilon}{\partial t}+\frac{\partial}{\partial x_j}\left(\rho u_j \varepsilon\right)=\frac{\partial}{\partial x_j}\left[\left(\mu+\frac{\mu_t}{\sigma_\varepsilon}\right)\frac{\partial \varepsilon}{\partial x_j}\right]+\rho\frac{\varepsilon}{k}\left(C_1\Pi-C_2\varepsilon+C_3\frac{\Pi^2}{\varepsilon}\right)$$

Gas-side Governing Equations - Continued

$$u^+ = \ln\left[\left(y^+ + 11\right)^{4.02} / \left(y^{+2} - 7.37\,y^+ + 83.3\right)^{0.79}\right] + 5.63\tan^{-1}\left(0.12\,y^+ - 0.441\right) - 3.81$$

$$T^+ = u^+ + 12.8\left(\mathrm{Pr}_l{}^{0.68} - 1\right)$$

$$Q_{cw} = \left(\rho\, u_\tau / T^+\right)\left[h_w - h_p - R\left(u_p{}^2 / 2\right)\right]$$

Conjugate Heat Transfer: Solid-side Governing Equations

Heat transfer in Solids

$$\frac{\partial \rho_s C_{ps} T_s}{\partial t} - \frac{\partial}{\partial x_j}\left(K_s \frac{\partial T_s}{\partial x_i} \right) = Q_v + Q_s$$

Gas / Solid Interface

$$\frac{1}{2}\rho C_p \frac{T_0^{'} - T_0}{\Delta t} = \frac{1}{\Delta x_j}\left(K \frac{T_1 - T_0}{\Delta x_j} - Q_s \right)$$

Conjugate Heat Transfer: Flow and Heat Transfer in Porous Media

Gas – Side Navier – Stokes and Energy Equations in Porous Media

$$\frac{\partial \rho u_i}{\partial t}+\frac{\partial}{\partial x_j}\left(\rho u_j u_i\right)=-\frac{\partial p}{\partial x_i}+\frac{\partial \tau_{ij}}{\partial x_j}-\frac{L}{\beta}$$

$$\frac{\partial \rho H}{\partial t}+\frac{\partial}{\partial x_j}\left(\rho u_j H\right)=\frac{\partial p}{\partial t}+Q_r+\frac{\partial}{\partial x_j}\left[\left(\frac{K}{C_p}+\frac{\mu_t}{\sigma_H}\right)\nabla H\right]+\frac{\partial}{\partial x_j}\left\{\left[(\mu+\mu_t)-\left(\frac{K}{C_p}+\frac{\mu_t}{\sigma_H}\right)\right]\nabla\left(\frac{V^2}{2}\right)\right\}+\theta+\frac{Q_s}{\beta}$$

Solid Heat Conduction in Porous Media

$$\frac{\partial \rho_s C_{ps} T_s}{\partial T}-\frac{\partial}{\partial x_j}\left(K_s\frac{\partial T_s}{\partial x_i}\right)=\frac{Q_v+Q_s}{1-\beta}$$

Detailed Flow Element Model

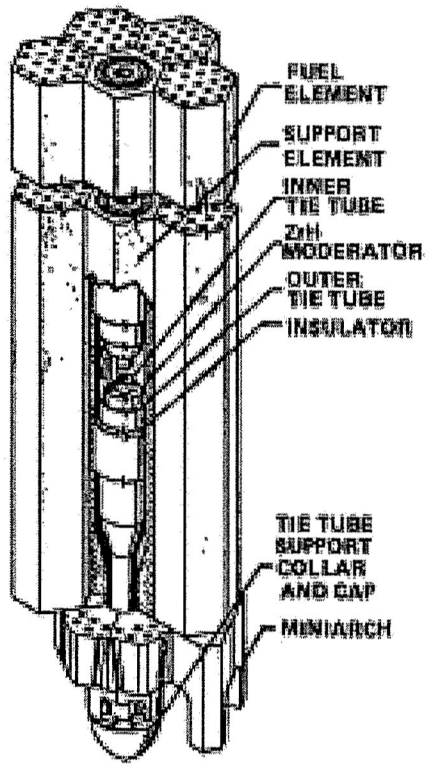

FUEL

- FUNCTION
  - PROVIDED ENERGY FOR HEATING HYDROGEN PROPELLANT
  - PROVIDED HEAT TRANSFER SURFACE
- DESCRIPTION
  - ^{235}U IN A COMPOSITE MATRIX OF UC-ZrC SOLID SOLUTION AND C
  - CHANNELS COATED WITH ZrO TO PROTECT AGAINST H_2 REACTIONS

TIE TUBES

- FUNCTION
  - TRANSMIT CORE AXIAL PRESSURE LOAD FROM THE HOT END OF THE FUEL ELEMENTS TO THE CORE SUPPORT PLATE
  - ENERGY SOURCE FOR TURBOPUMP
  - CONTAIN AND COOL ZrC MODERATOR SLEEVES
- DESCRIPTION
  - COUNTER FLOW HEAT EXCHANGER OF INCONEL 718
  - ZrH MODERATOR
  - ZrC INSULATION SLEEVES

Fig. 41. Description of the Small Engine fuel module design showing the ZrH sleeve in the regeneratively cooled tie-tube support element.

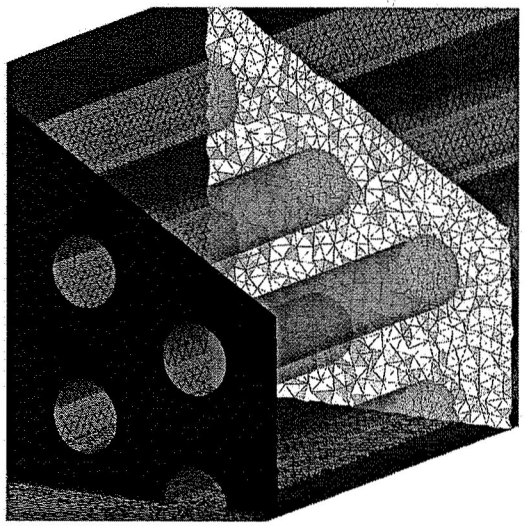

Small Engine Flow Element Bundle

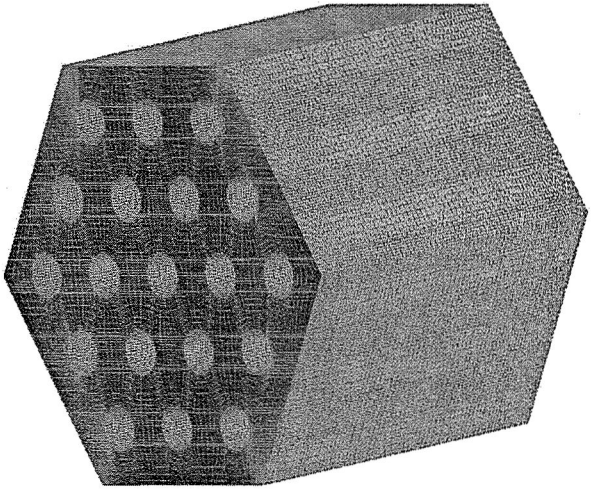

19-channel Flow Element Model

Global Thrust Chamber Model

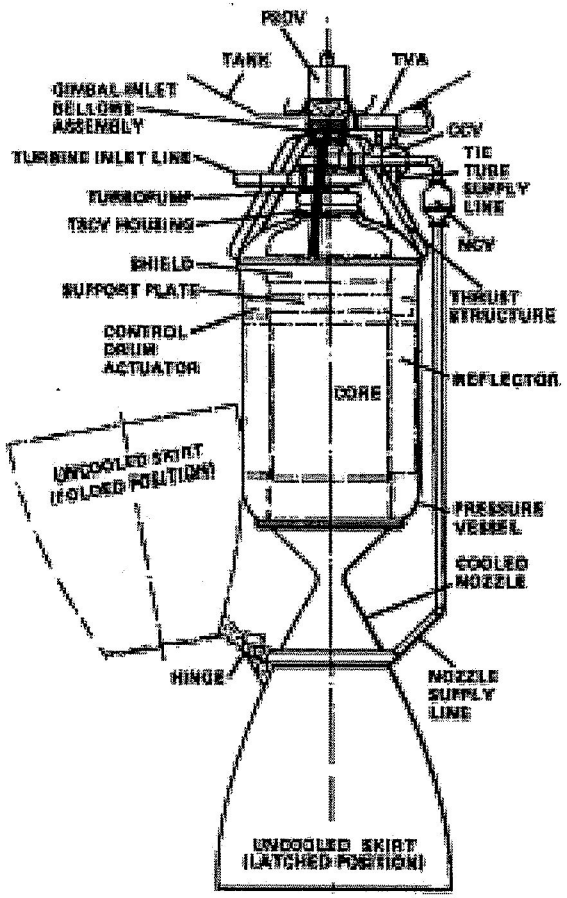

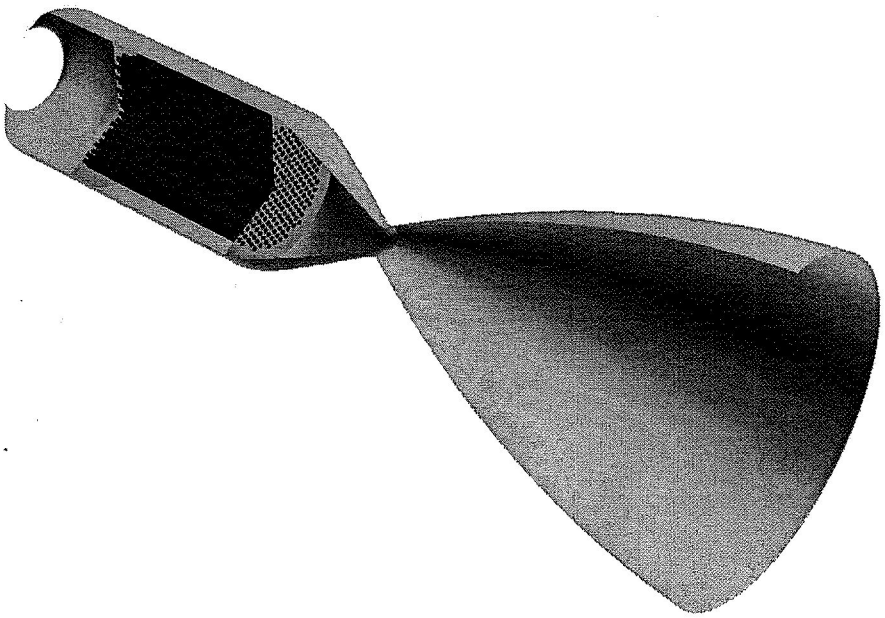

Small Engine

Thrust Chamber Model

Global Thrust Chamber Model

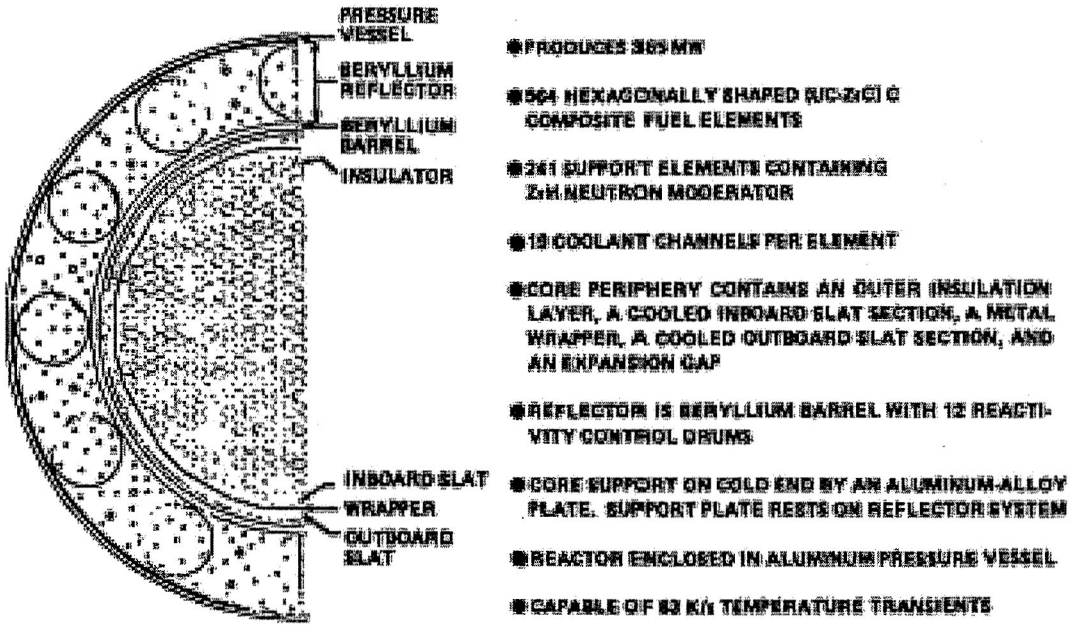

Fig. 40. Cross-sectional description of the Small Engine concept. The overall reactor diameter was 950 mm. The design used ZrH-moderated support elements, as was done in Pewee, to reduce the uranium critical mass.

Small Engine Solid-core

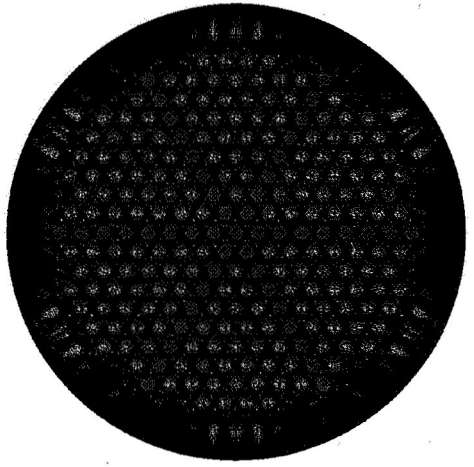

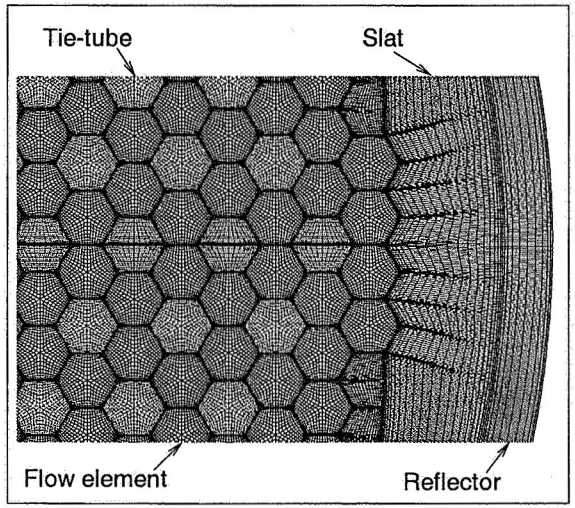

Thrust Chamber Model

Result of Detailed Flow Element Analysis
1/8 Full-Length

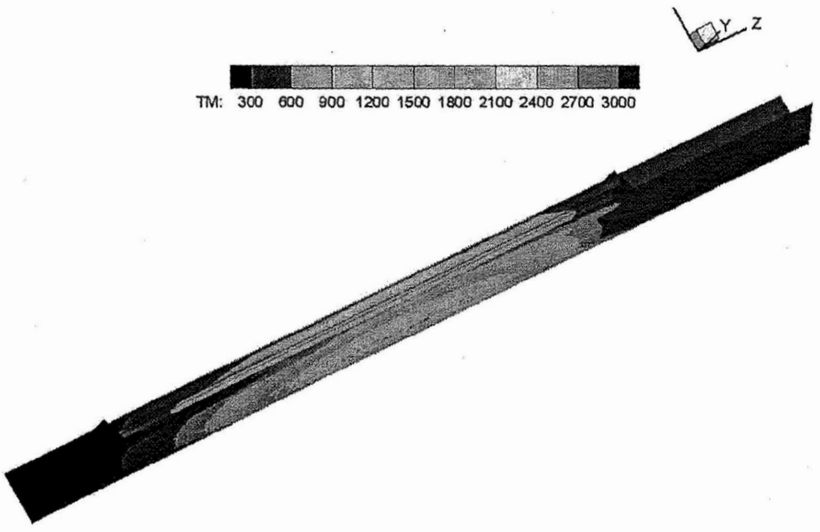

Computed temperature contours

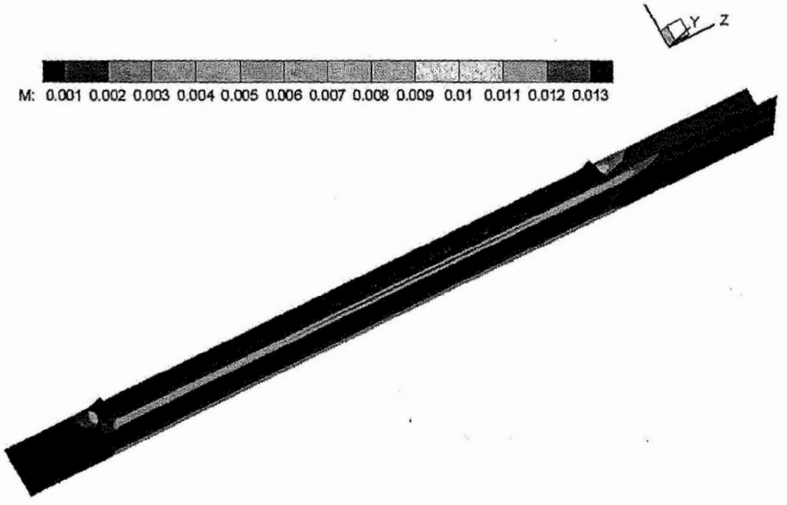

Computed Mach number contours

Result of Global Thrust Chamber Analysis

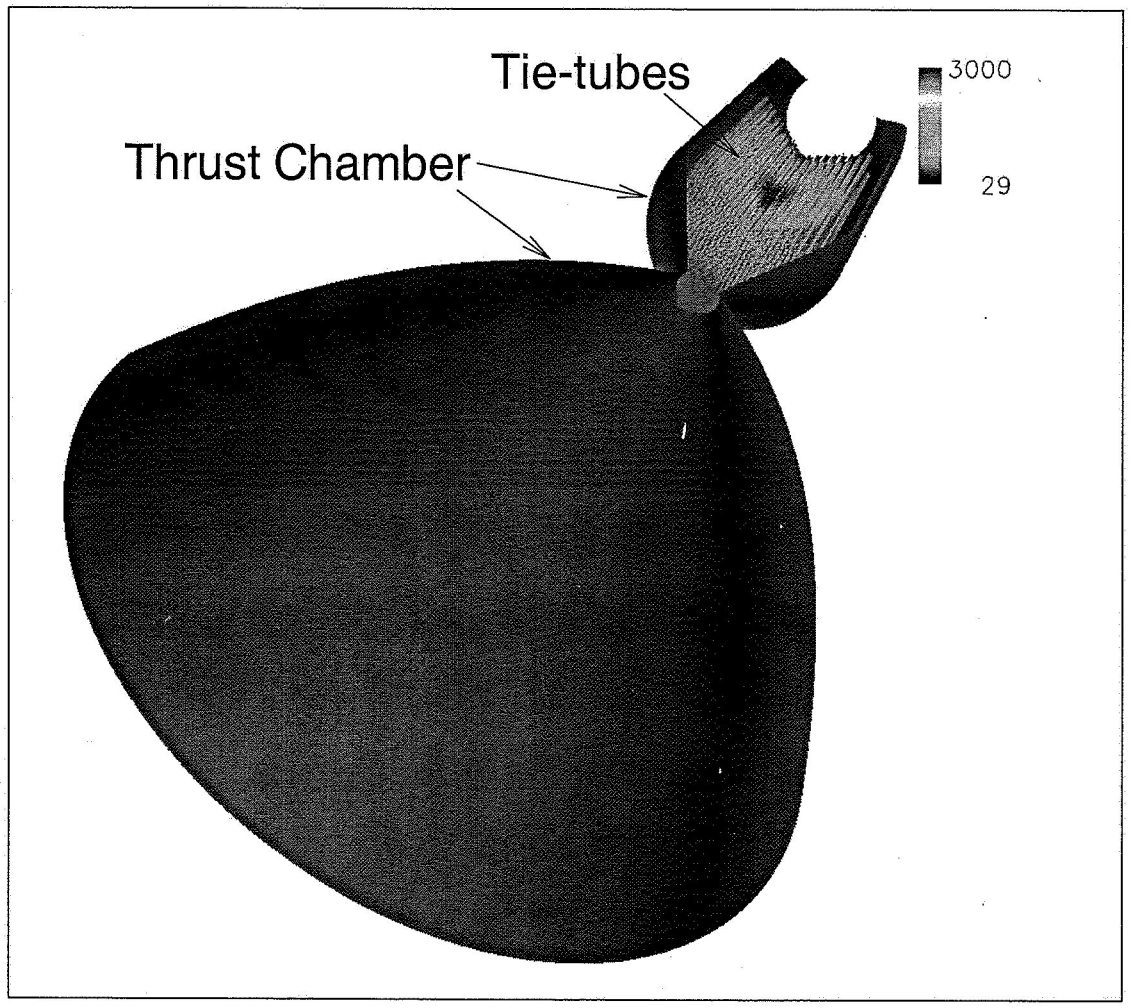

Computed temperature contours

Result of Global Thrust Chamber Analysis

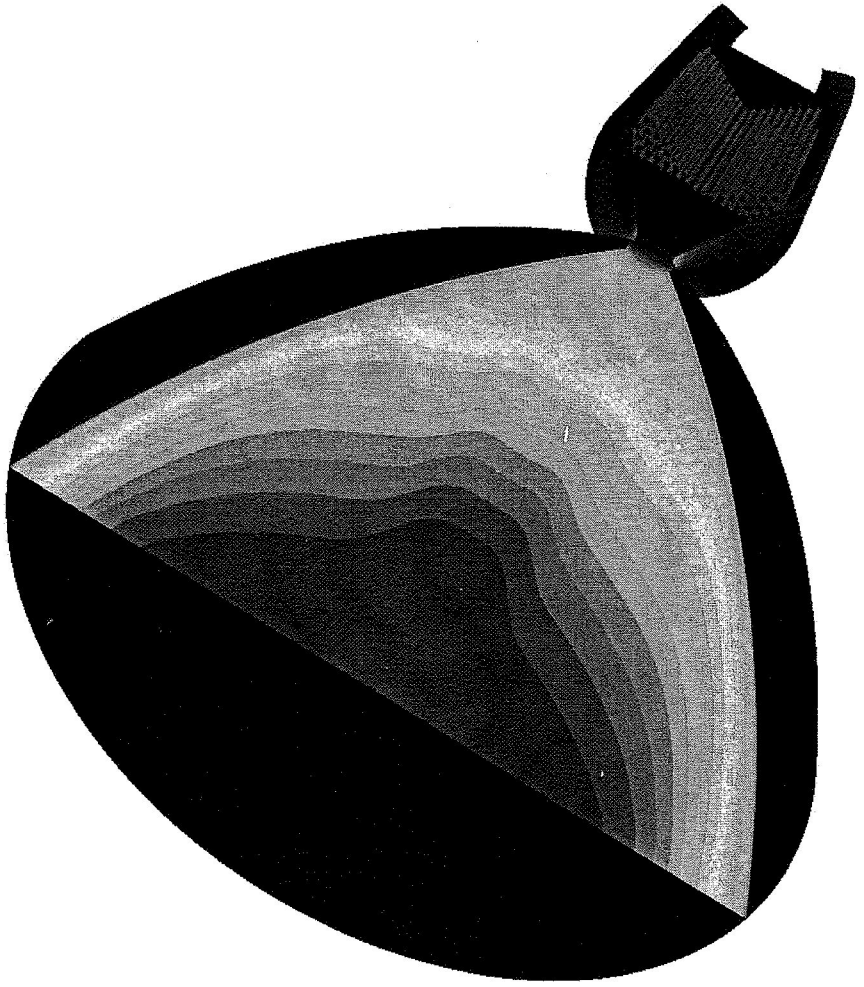

Computed pressure contours on thrust chamber and tie-tube walls,
and Mach number contours on symmetry plane

Summary

- A computational conjugate heat transfer methodology was developed to predict environments for a hypothetical solid-core, nuclear thermal engine thruster and the associated flow element.
- A two-pronged approach was employed: A detailed analysis on a 19-channel flow element for mid-section corrosion investigation; and a global analysis on a thrust chamber to understand the effect of hydrogen dissociation and recombination on heat transfer efficiency and thrust performance.
- The computed thermal-fluid-hydrogen environments in the flow element and thrust chamber appear to be reasonable.